Transactions of the Materials Research Society of Japan 29 [8] 3603-3606 (2004)

Crack Growth Mechanism in Iron under Cyclic Loading

Kenji Nishimura and Noriyuki Miyazaki*
National Institute of Advanced Industrial Science and Technology (AIST),
Tsukuba Central 2, Tsukuba, 305-8568, JAPAN
Fax: 81-29-861-3170, e-mail: k.nishimura@aist.go.jp
*Kyushu University, 6-10-1 Hakozaki, Higashi-ku, Fukuoka, 812-8581, JAPAN
Fax: 81-92-642-3531, e-mail: miyazaki@apex.chem-eng.kyushu-u.ac.jp

The mechanical behaviors around a crack tip at an atomic scale level under cyclic loading are examined using a molecular dynamics simulation. In this study, we deal with not only a specimen including both a crack and grain boundaries but also a specimen including only a crack. For the specimen including both a crack and grain boundaries, we can observe the emission of edge dislocations in order to relax stress concentration around the crack tip during loading. The dislocations emitted from the crack tip return to the crack tip because of interaction between dislocations during unloading. The crack propagates due to coalescence of the crack tip and the vacancies caused by the repeat of the dislocation emission and absorption at the crack tip. For the specimen including only a crack, the emission of edge dislocations from the crack tip is observed during the first loading. Then, a slip deformation occurs in the specimen after the dislocations reach a free surface. The crack does not propagate because of plastic blunting at the crack tip due to the emission of the dislocations.
Key words: Molecular dynamics method, Fatigue crack growth, Dislocation, Grain boundary, iron

1. INTRODUCTION

The essence of fatigue crack growth is that the process includes the plastic deformation at a micro scale level. In order to examine the fatigue crack growth accompanied by the plastic deformation, many investigations have been carried out experimentally [1-4]. On the other hand, many computer simulations at an atomistic scale have been performed to clarify the fracture mechanism under monotonic loadings. Cleri *et al.* [5] dealt with crack-tip shielding by dislocations emitted from the crack tip at an atomistic level under monotonic loadings using a molecular dynamics simulation. Large scale molecular dynamics simulations by the use of three dimensional model were performed to investigate the emission of dislocation loops from the crack tip and dislocation intersections [6, 7]. Moreover, a molecular dynamics method has been applied to a system including both a crack and a grain boundary. Nishimura and Miyazaki [8] reported the effect of a grain boundary on the brittle crack propagation in α-Fe. As shown above, the molecular dynamics method has been successfully applied to simulate the mechanical behaviors of materials under monotonic loadings. However, few studies on the application of the molecular dynamics simulation to the fatigue damage were reported because a fatigue simulation is a time-consuming task. Chang [9] obtained relationship between the cyclic stress and number of cycles to failure for nanoscale copper from the fatigue simulations of a system including vacancies. In the present study, we perform the molecular dynamics simulation of systems with one million atoms using a pair potential developed by Johnson for α-Fe to clarify the fracture of materials including grain boundaries together with the process of plastic deformation under cyclic loading.

2. METHOD OF ANALYSIS

Fig. 1 shows the relationship between a crystallographic orientation and a coordinate system of a crack. We deal with the in-plane opening or mode I deformation of the crack due to the limitation of the number of atoms, although a fatigue crack propagates in the mode II or mode III experimentally. The {110} plane is a close-packed plane for the bcc structure, and the slip plane and the slip direction of the structure

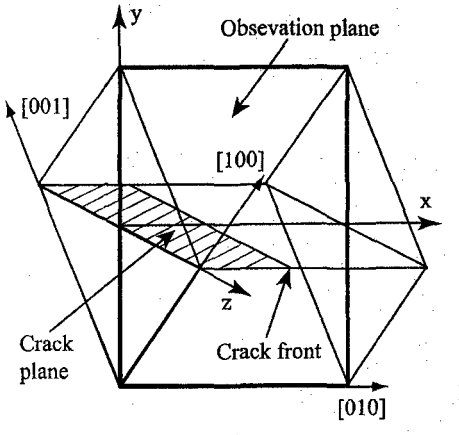

Fig.1 Relationship between a crystallographic orientation and a coordinate system of a crack.

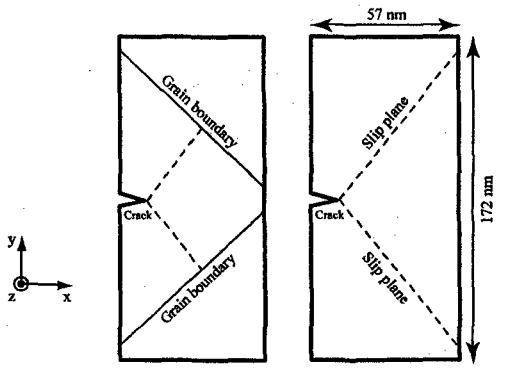

Fig.2 Schematic diagrams of specimens for a molecular dynamics simulation.

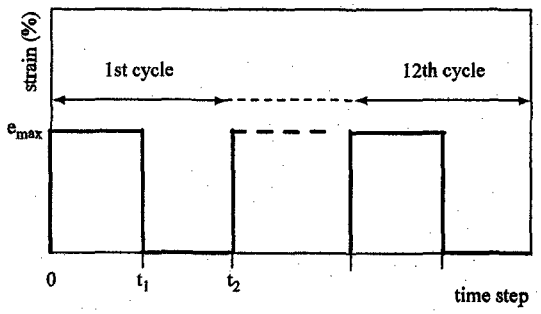

Fig.3 Loading pattern subjected to the specimens.

correspond to the {112} plane and <111> direction, respectively. The close-packed (10$\bar{1}$) plane indicated by bold lines in Fig. 1, which includes the slip direction, is used as an observation plane, at which the results of the molecular dynamics simulation are shown. The crack direction is the [010] direction in the (101) plane as shown in Fig. 1.

In the molecular dynamics method, a material is modeled as a multi-particle system governed by the classical mechanics. The particles or atoms move by summing up inter-atomic forces exerted from other atoms, and the motion of the atoms is expressed by the Newton's law of motion. It is considered that the use of a pair potential as a function of a distance between two atoms is simple and convenient in order to describe the inter-atomic forces in α-Fe. We use the Johnson potential [10], from which the lattice constant and elastic constants of α-Fe at the temperature of 0 K are reproduced.

Schematic diagrams of specimens for a molecular dynamics simulation are shown in Fig. 2. We deal with two specimens in this study. One specimen includes both a crack and two grain boundaries and another specimen includes only a crack, as shown in Fig. 2 (a) and Fig. 2 (b), respectively. The lengths of the x-direction and y-direction are 57 nm and 172 nm, respectively. Initially we allocate atoms at the bcc lattice positions and give the velocities of the atoms which follow the Maxwell distribution at a prescribed temperature of 300 K. The specimens consist of about one million atoms.

Fig. 3 shows a loading pattern subjected to the specimens. We apply twelve rectangular cyclic loadings to the specimens. The specimen is stretched rapidly after relaxation at a strain level of 0 %. After the strain is applied to the specimen, we use a canonical ensemble which keeps the volume and temperature of the system constant. Then, the stain level returns to 0 % and the calculation for relaxation is carried out. We repeat the same process twelve times. We observe not only the time evolution of a stress distribution in the specimen but also atom configurations around the crack tip after loading and unloading.

There have been a lot of studies using the molecular dynamics simulation on the evaluation of grain boundary energy and on the grain boundary structure. Wolf [11] calculated the grain boundary energy of a symmetrical tilt grain boundary in α-Fe by changing misorientation angle. As a result, several local minimum points of grain boundary energy appear with increasing the misorientation angle. The lowest grain boundary energy is 200 mJ/m^2 around 110 degrees of the misorientation angle and the grain boundary plane is the {112} plane. This grain boundary is considered in this study. The shape of the structural unit of the grain boundary is almost the same as that in bulk region. Moreover, the grain boundary shows good lattice consistency and coherency.

3. SIMULATION RESULTS AND DISCUSSION

3.1 In the case of a specimen including both a crack and grain boundaries

Fig. 4 shows an atom configuration around a crack tip at 1200 time steps after the first loading is applied to the specimen 1. The atoms in the two layers of z-direction are shown in the figure, where the black atoms and white ones indicate that they exist in different layers, respectively. Around the crack tip, there is a diamond-shaped domain surrounded by a solid line, where the crystal structure differs from bcc. In this domain, we can observe hexagonal atomic structure like stacking triangle lattices. We also confirm that the stacking structure of the z-direction is ABABAB. Since Bancroft *et al.* [12] discovered the bcc to hcp phase transition of iron in 1956, a lot of knowledge on the phase transition has been obtained through numerous investigations. Wang and Ingalls [13] measured the

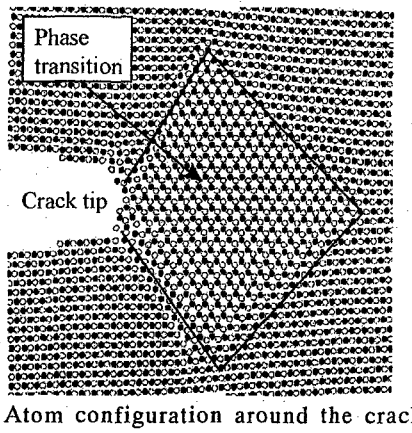

Fig.4 Atom configuration around the crack tip at 1200 time steps after the first loading is applied to the specimen 1.

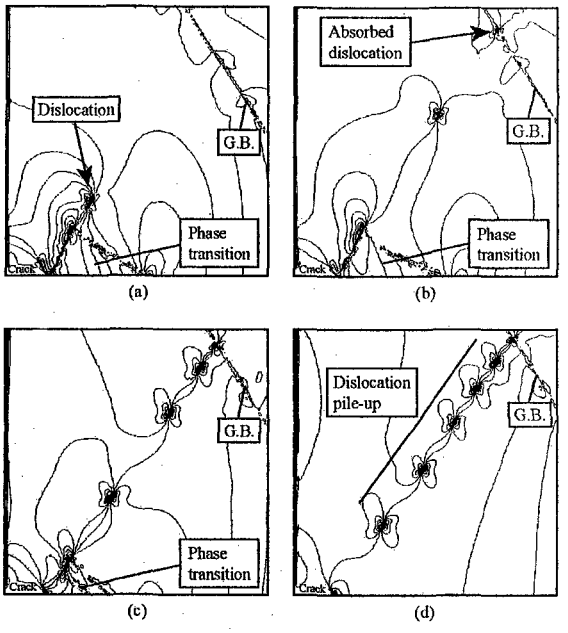

Fig.5 Time evolution of the distribution of the local stress σ_y between the crack tip and the grain boundary in specimen 1 during the first loading.

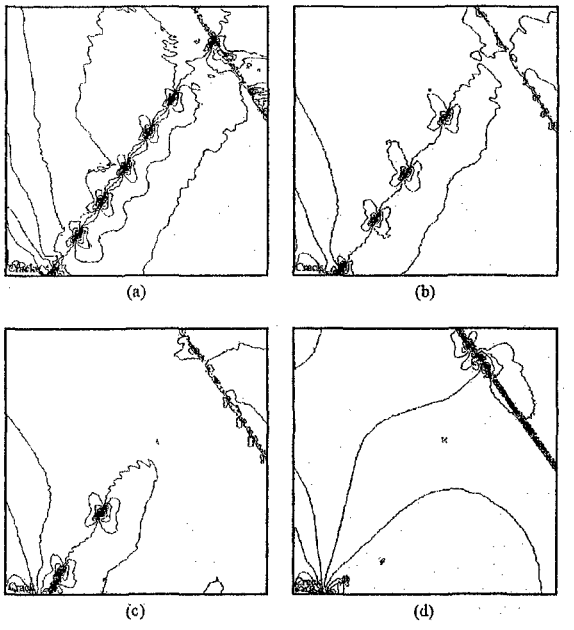

Fig.6 Time evolution of the distribution of the local stress σ_y between the crack tip and the grain boundary in specimen 1 during the first unloading.

lattice constant and c/a ratio of ε-Fe which has hcp structure. Cheung *et al.* [14] performed molecular dynamics simulations to examine the mechanism of the phase transition induced by uniaxial tensile stress. Considering the previous studies mentioned above, we can conclude that the domain around the crack tip whose crystal structure differs from bcc is the hcp phase induced by high stress which results from stress concentration around the crack tip. Hereafter we call it a phase transition domain.

The time evolution of the distributions of the local stress σ_y between the crack tip and the grain boundary during the first loading is shown in Fig. 5 (a) through Fig. 5 (d). A crack is located at the corner of the lower left. In Fig. 5 (a), the phase transition from bcc to hcp as mentioned above is observed. Moreover, we can observe an edge dislocation at the upper right-hand side of the crack tip. The slip direction and slip plane of the edge dislocation correspond to the [111] direction and the $(1\bar{2}1)$ plane, respectively, which agree with the slip system of α-Fe. Then, the dislocation emitted from the crack tip glides in the slip direction and is absorbed into the grain boundary after it reaches the grain boundary, as shown in Fig. 5 (b). The emission of the edge dislocations from the crack tip continues in Fig. 5 (c). We can confirm from this figure not only the shrinkage of the phase transition domain caused by the emission of the edge dislocations but also the formation of dislocation pile-up starting from the grain boundary because the edge dislocations cannot move beyond the grain boundary after they reach it. Finally, the dislocation pile-up as a stable structure is formed and the phase transition domain disappears, as shown Fig. 5 (d).

The time evolution of the distributions of the local stress σ_y between the crack tip and the grain boundary during the first unloading is shown in Fig. 6 (a) through Fig. 6 (d). We can observe that the dislocations forming the dislocation pile-up near the grain boundary return to the crack tip rapidly after unloading due to interaction between dislocations, as shown in Figs. 6 (a), (b) and (c). In Fig. 6 (d), all dislocations return to the crack tip and dislocations disappear in the specimen.

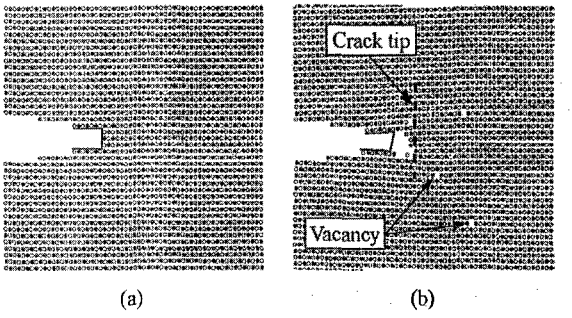

Fig.7 Atom configurations around the crack tip in specimen 1: (a) before cyclic loading; and (b) after the twelfth cycle.

When the loading and unloading are repeated, the emission and absorption of the dislocations at the crack tip observed during the first cycle are repeated. We compare the initial atom configuration before cyclic loading with the final atom configuration after twelfth cycle in Fig. 7. The initial and finial crack fronts are shown in Figs. 7 (a) and (b) as a solid line and a dotted line, respectively. We can observe not only crack propagation but also vacancies generated around the crack tip in Fig. 7 (b). Moreover, we can find from this figure that after twelfth cycle the crack growth length is 1.3 nm, hence the crack growth rate is 0.11 nm/cycle.

From what has been discussed above, we would like to propose the fatigue crack growth mechanism for the

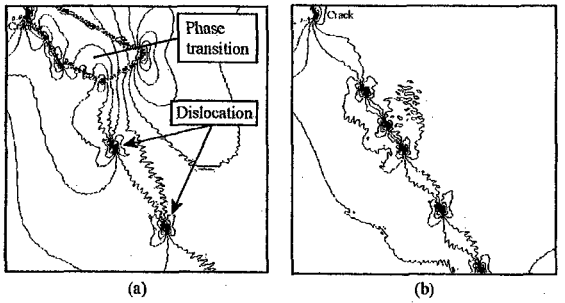

Fig.8 Time evolution of the distribution of the local stress σ_y around lower right hand side of the crack tip in specimen 2 during the first loading.

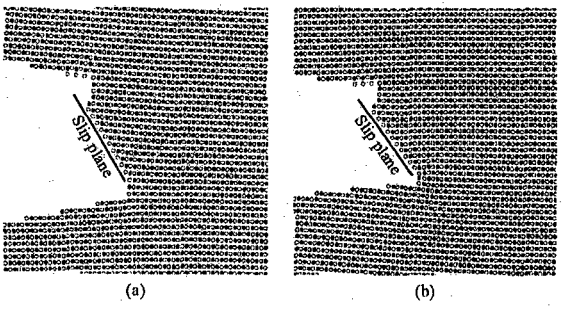

Fig.9 Atom configurations around the crack tip in specimen 2: (a) after the first loading; and (b) after the first unloading.

initial phase of the fatigue fracture. From our simulation in this study, plastic deformation such as dislocation emission from the crack tip during loading and dislocation absorption into the crack tip during unloading are observed. Furthermore, the repeat of both dislocation emission and absorption at the crack tip under cyclic loading causes the formation of vacancies around the crack tip. As a result, the crack propagates due to coalescence of the vacancies and the crack tip.

3.2 In the case of a specimen including only a crack

The time evolution of the distributions of the local stress σ_y around lower right hand side of a crack tip in specimen 2 during the first loading is shown in Figs. 8 (a) and (b). We can observe not only the phase transition domain but also the edge dislocations emitted in Fig. 8 (a), as mentioned above. Then, the phase transition domain shrinks and disappears at the crack tip whereas a lot of dislocations are emitted from the crack tip. Because the specimen does not include obstacles to the motion of the dislocations such as grain boundaries, the dislocations can reach a free surface, opposite side of the crack tip. The disappearance of the dislocations causes deformation like stairs at the free surface.

Figs. 9 (a) and (b) show atom configurations around the crack tip after the first loading and the first unloading, respectively. As a result of dislocation emission, the generation of a slip plane at the crack tip is observed after the first loading in Fig 9 (a). Indeed the crack opening decreases, but the shape of the crack tip hardly changes and the slip plane remains after the first unloading, as shown in Fig. 9 (b). Although we apply five cyclic loadings to the specimen, we cannot observe either plastic deformation process such as dislocation emission or crack propagation. Conclusively, the plastic blunting prevents both the plastic deformation and the crack propagation because stress concentration does not occur at the crack tip.

4. CONCLUSIONS

We have performed a molecular dynamics simulation of α-Fe to examine the mechanical behaviors at an atomic scale level under cyclic loading. We dealt with not only a specimen including both a crack and grain boundaries but also a specimen including only a crack. In the case of the specimen including both a crack and grain boundaries, we can observe the emission of edge dislocations from the crack tip during loading. During unloading the dislocations emitted from the crack tip return to the crack tip because of interaction between dislocations. The crack propagates due to coalescence of the crack tip and vacancies formed by the repeat of the dislocation emission and absorption at the crack tip. In the case of the specimen including only a crack, the emission of edge dislocations from the crack tip is observed during the first loading. Then, a slip deformation occurs in the specimen after the dislocations reach a free surface. The crack does not propagate because of the plastic blunting of the crack tip due to the emission of the dislocations.

ACKNOWLEDGEMENTS

This work was supported by NAREGI Nanoscience Project, Ministry of Education, Culture, Sports, Science and Technology, Japan.

REFERENCE

[1] H. Vehoff and P. Neumann, *Acta Metal.*, **27**, 915-920 (1979).
[2] S. M. Ohr, *Mater. Sci. Eng.*, **72**, 1-35 (1985).
[3] S. E. Harvey, P. G. Marsh and W. W. Gerberich, *Acta Metal. Mater.*, **42**, 3493-3502 (1994).
[4] M. Jono, Y. Sugeta and Y. Uematsu, *Fatigue Fract. Eng. M.*, **24**, 831-842 (2001).
[5] F. Cleri, S. Yip, D. Wolf and S. R. Phillpot, *Phys. Rev. Lett.*, **9**, 1309-1312 (1997).
[6] S. J. Zhou, B. M. Beazley, P. S. Lomdahl and B. L. Holian, *Phys. Rev. Lett.*, **78**, 479-482 (1997).
[7] F. F. Abraham, R. Walkup, H. J. Gao, M. Duchaineau, T. D. De la Rubia and M. Seager, *P. Natl. Acad. Sci. USA*, **99**, 5783-5787 (2002).
[8] K. Nishimura and N. Miyazaki, *CMES-Comp. Model. Eng.*, **2**, 143-154 (2001).
[9] W. J. Chang, *Microelectronic Eng.*, **65**, 239-246 (2003).
[10] R. A. Johnson, *Phys. Rev. A*, **134**, 1329-1336 (1964).
[11] D. Wolf, *Philos. Mag. A*, **62**, 447-464 (1990).
[12] D. Bancroft, E. L. Peterson and S. Minshall, *J. Appl. Phys.*, **27**, 291-289 (1956).
[13] F. M. Wang and R. Ingalls, *Phys. Rev. B*, **57**, 5647 -5654 (1997).
[14] K. S. Cheung, R. J. Harrison and S. Yip, *J. Appl. Phys.*, **71**, 4009-4014 (1992).

(Received October 10, 2003; Accepted April 23, 2004)